Influence of Twinning on the Morphology of AgBr and AgCl Microcrystals

W. Van Renterghem, C. Goessens,* D. Schryver▲, and J. Van Landuyt
EMAT, University of Antwerp, Antwerpen, Belgium

D. Bollen, R. De Keyzerˢ and C. Van Roost
Agfa-Gevaert N.V., Mortsel, Belgium

An overview is given of non-tabular crystals with {111} surfaces occurring in emulsions of silver bromide and silver chloride tabular grains. The crystal defects are characterized by transmission electron microscopy (TEM) and their influence on the growth process is discussed. It is proven that in all cases of non-tabular growth twins on two non-parallel {111} type planes are present. Different morphologies have been observed in AgBr and AgCl emulsions. The most frequently occurring morphologies are needle and tetrahedron shaped crystals in AgBr and thick tabular crystals with an incomplete microtwin as well as crystals consisting of a tetrahedral shaped part and a flat triangular to trapezoidal part in AgCl. A comparison will be made between the silver bromide and the silver chloride crystals.

Introduction

Silver halide microcrystals, where the halide stands for chloride or bromide, are used as the light sensitive element in photographic films. Silver bromide and chloride have the same crystal structure as NaCl, and if no defects or growth modifying agents are introduced cubic or octahedral crystals are formed. However, precipitation of AgBr crystals at high supersaturation, e.g. at high bromide concentration, results in twinning along {111} type planes[1,2] inducing lateral growth. Under these conditions, populations of silver bromide crystals mostly consist of tabular crystals,[3] and in every tabular crystal, two or three twin planes parallel to the basal plane are present.[4]

Much has been written about the effect of twinning on the enhanced growth rate of crystals. Twins in grown diamond films were observed to enhance the growth in the direction lying in the twin plane.[5,6] Flat, hexagonal shaped diamond platelets were observed during the initial stage of microwave plasma assisted deposition of diamond.[7] A re-entrant groove was seen to be present in the small side faces of the platelets, at which preferential adsorption of growth material occurs. Also in C_{60}[8] and in gold and silver particles, prepared by the solution reduction of either chloroauric acid or silvernitrate with citric acid, plate-like morphologies were observed.[9] Hamilton and Seidensticker[10] proposed a model for the enhanced lateral growth of twinned platelets. A key feature for the rapid growth was argued to be the re-entrant groove between two adjacent {111} type planes at the twin plane.

This model[10] is also used to explain the growth characteristics of twinned silver halide crystals. Jagannathan[11] calculated for silver bromide crystals a probability of adsorption of a growth species at the re-entrant groove that is about 50 times higher with respect to adsorption at a surface site. An isolated atom at a surface site on a (111) plane has three nearest neighbors, while it has four at the re-entrant groove, resulting in a stronger bonding, thus explaining the difference in growth rate. Ming and co-workers[12,13] came to the same conclusion using Monte Carlo simulations. They showed the twin lamella to act as self-perpetuating sites of enhanced nucleation.

Later it was argued that the side faces are built up by {111} and {100} faces[11,14]. These {100} faces grow at higher rate than the {111} faces. The substep-mechanism developed by Ming and co-workers[12,15] explains how the entire side face grows as fast as the {100} part. Therefore the {100} faces do not disappear and the anisotropic growth is continued. Recent experiments[16,17] appear to confirm the second growth model. For AgBr, it is possible to produce populations that contain more than 97% of tabular crystals.

It is not possible to produce AgCl tabular crystals in the same way as for AgBr because, due to the high ionic charges, the {111} surfaces of a silver chloride crystal are not stable in an aqueous environment. One solution to overcome this problem is the production of tabular crystals with {100} surfaces. For these crystals, the introduction of mixed dislocations that extend in two directions parallel to one of the {100} surfaces was proven responsible for the anisotropic growth.[18]

A second solution is the addition of a stabilizer for the {111} surfaces. Different stabilizers have been tested,[19,20] with adenine giving the best results and being most often used. However, when precipitated under the same conditions as for AgBr, still 10 to 30% of the AgCl crystals also grow in the third dimension, despite the addition of adenine. In this article, the existence of extra lattice defects in thick crystals occurring in AgBr and AgCl emulsions is documented and models for their effects on the thickness growth are presented.

Experimental

The AgBr emulsion was prepared by the standard double jet method. The initial concentrations in solution were 0.55 mole/L of KNO_3, 0.015 mole/L of KBr and 5.77 g/L of gelatin in a volume of 500 ml. Nucleation was performed at 50°C with addition rates of 6 ml/min for 60 sec. The temperature was then raised to 70°C during 20 min. The silver addition rate increased during growth from 1.5 to 3.5 ml/min with a constant gradient. The addition rate of KBr was permanently adjusted to maintain the free silver ion concentration at the initial value. The sample was desalted by flocculation and the gelatin was separated from the crystals by centrifugation.

For the AgCl emulsion again the standard double jet method was used. $AgNO_3$ and NaCl are added to a mixture of gelatin, water and an adequate amount of adenine for the stabilization of the {111} surfaces. The growth procedure is started with a nucleation phase at high super-saturation to introduce the twins necessary for the tabular growth followed by a physical ripening and a long growth phase with increasing addition rate. The crystals are produced at a temperature of 55°C in the nucleation phase and are ripened and grown at 70°C. The pH was fixed at 6.0 during the entire growth process. A decrease of the pH below 5.5 leads to desorption of adenine from the surface, which results in the loss of the stability of {111} surfaces, and hence no tabular grains are formed.

For the preparation of the samples for TEM investigation, 50 µl of the emulsion is diluted in 50 ml of distilled water. A drop of this mixture is placed on a copper grid, covered with a carbon foil. The microscopes used for this investigation are a Philips CM20 and a Philips CM200 instrument both using an accelerating voltage of 200 kV. In order to avoid radiation damage the preparation of the specimens and the mounting in the microscope are performed under red light conditions and during examination the samples were cooled with liquid nitrogen in a Gatan double tilt-cooling holder. The working temperature was approximately 100 K.

Results

In emulsions precipitated at high pAg values, most crystals have two or three parallel (111) twin planes, resulting in thin tabular sheet crystals with a triangular or hexagonal form. However, a minority of the total population of crystals shows different morphologies, less than 3% for AgBr and 10 to 30% for AgCl when produced under similar growth conditions. These different morphologies are in all cases the result of the formation of non-parallel twins. Four different kinds of morphologies will be discussed here, i.e., needle shaped crystals and tetrahedrons that occur in AgBr emulsions and thick crystals with an incomplete microtwin and tricrystals that occur mainly in AgCl emulsions. The characterization of the defects will not be elaborated on
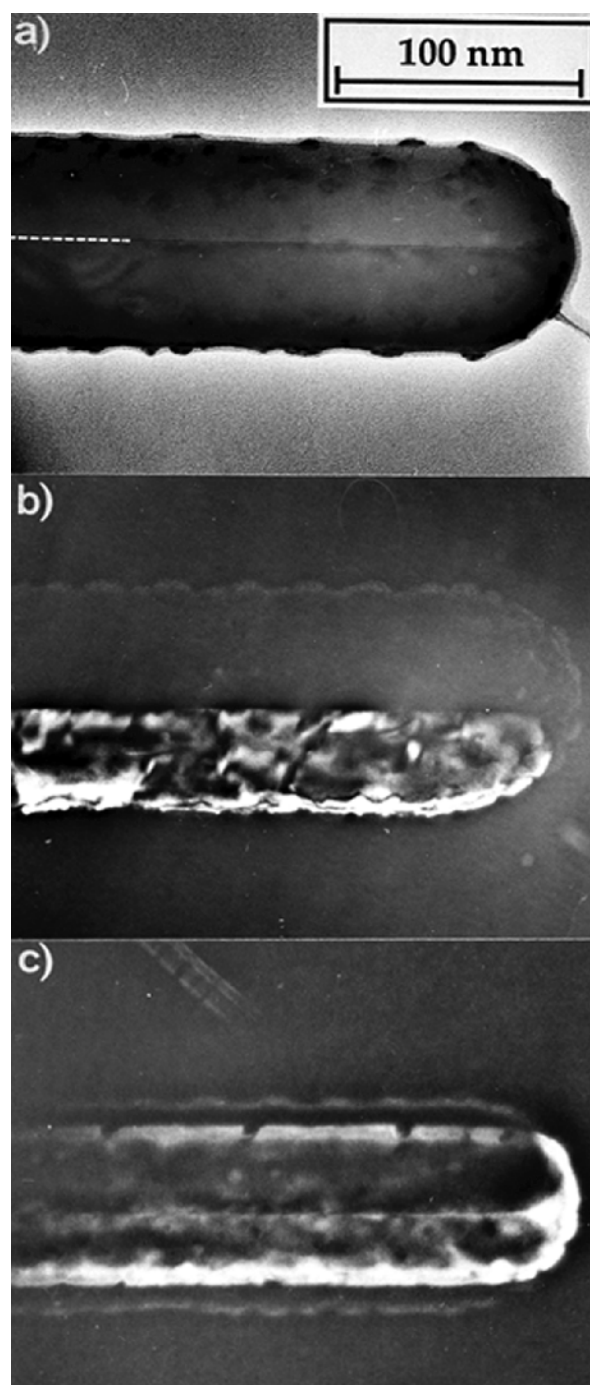

Figure 1. a) Bright field TEM image of a needle crystal. The dark line of contrast indicates the location of the {221} twin plane; b) dark field image of the same needle using the 200 reflection of a first variant; c) dark field image of the same needle using the 200 reflection of a second variant.

in detail, but can be found in the articles of Goessens and co-workers[21,22] and Van Renterghem and co-workers.[23] This article will focus on the comparison between the thick crystals in AgBr emulsions and thick crystals in AgCl emulsions.

AgBr: Needles and Tetrahedrons

In Figs. 1a–c a typical image of a needle shaped crystal is shown. The diameter of the needles (about 100–
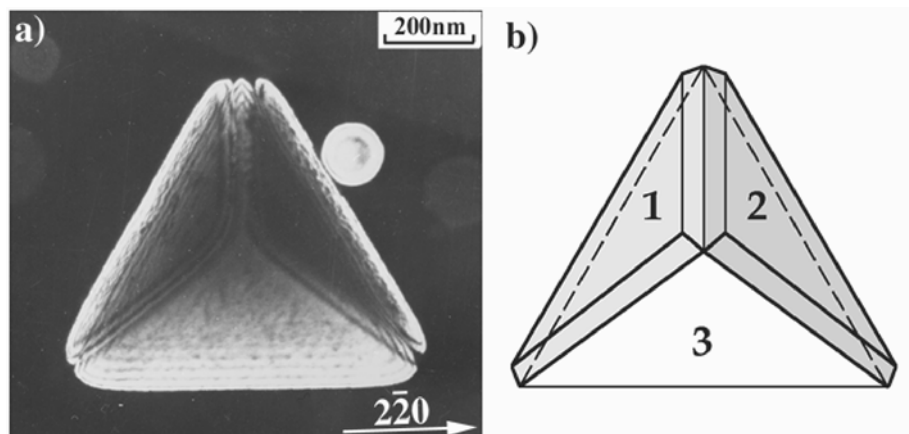
Figure 2. a) Dark field TEM image and b) drawing of a tetrahedral shaped crystal. The grey areas indicate the location of the twinned variants.

150 nm) was found to be of the same order of magnitude as the lateral size of the tabular microcrystals after the physical ripening, after which the latter grow to become tabular crystals. This indicates that the growth of the needles only occurs along the long edge of the crystal and that growth in all other directions is inhibited. The length is about ten times the diameter of the tabular crystals after the precipitation, indicating a unilateral growth that is about ten times faster than the growth of tabular crystals. From an analysis of diffraction patterns and dark field images (Fig. 1b–c) it was determined that three twin variants are present separated by three interfaces. Two of them are {111} type twin planes enclosing an angle of 109.5°. The third is a twin lying on a {221} plane that is the result of the existence of the two {111} type twin planes.

A second kind of morphology related to the occurrence of non-parallel twinning of {111} type planes is shown in Fig. 2. The crystals show in transmission a triangular morphology, and their size is typically 400 nm or more, i.e., larger than the width of the needle crystals discussed above, to such an extent that in most crystals transmission of the electron beam is greatly hampered by absorption. However, the thickness is not uniform, and some parts of the crystals are thin enough to result in observable diffraction spots. This is consistent with the contrast fringes observed near and parallel to all edges of the crystal in Fig. 2, which indicates an increasing thickness when going from the edge of the crystal to the central part.

Apart from the thickness fringes, triangular darker regions are observed at two of the three edges of the crystal. The two regions of darker contrast can be readily interpreted as being the result of the presence of two twin related variants on top of the central variant. The two twin related variants are inclined over an angle with respect to the electron beam while the central larger variant exhibits a more uniform contrast. From tilting experiments and examining the thickness fringes in the central variant, it can be seen that this variant has a tetrahedral morphology, while the other two variants are thin twinned slabs with a typical thickness of a few tens of nm. This results in morphology of the entire crystal that is almost tetrahedral.

The drawing in Fig. 2b corresponds well to the image shown in Fig. 2a. The larger, central variant is in contact with two twin-related, thin slabs, enclosing an angle of 70.5° with each other. As in the case of the nee-

dle crystals, an extra mirror plane is introduced due to the (111) type twinning. In this case, it is a {411}-type plane. However, the presence of this extra mirror plane is only a result of the existence of the {111} type twin planes, i.e., it is an effect of second order.

AgCl: Crystals with an Incomplete Microtwin and Tricrystals

A typical example of a crystal with a microtwin terminating inside the crystal is shown in Fig. 3. An analysis of diffraction patterns generated by these crystals showed that three twin related variants are present. The interfaces between the variants are twin planes, lying on the (111) plane parallel to the tabular surfaces and on a non-parallel {111} plane. The dark field image of Fig. 3a shows a fringe contrast (arrow) caused by one or more planar defects. Using a reflection excited in the third variant, only the area of the fringes in Fig. 3a is bright. This reveals the configuration of the third variant limited by two parallel planes. From the analysis of the crystallography, it can be concluded that the defect responsible for the fringe contrast and lighting up in the dark field images is a microtwin. It is remarkable that the microtwin ends inside the crystal. Arguments based on Monte Carlo simulations[24] have been given to account for this observation.

The analysis of all diffraction patterns generated in these crystals shows that no other twin variants are formed. This means that the non-parallel twins are formed in only one variant. This can be concluded from Fig. 6 in a previous article by Van Renterghem co-workers.[23] In this diffraction pattern three different twin related variants generate three sets of reflections. The first variant is oriented along the [234]-zone, the parallel twin along the [432] zone and the non-parallel twin along the [052] zone. If also non-parallel twins would be formed in the second, parallel twinned variant, then a fourth set of reflections should appear oriented along the [250] zone. No reflections belonging to this zone could be observed, indicating that the non-parallel twin is formed in only one variant. This is in contrast with the conclusion from diffraction contrast images of tabular AgBr/AgBrI core–shell crystals showing stacking faults or microtwins in all twin variants,[25] although Chen co-workers[26] only observed microtwins in the outer variants of such crystals after cross-sectioning.

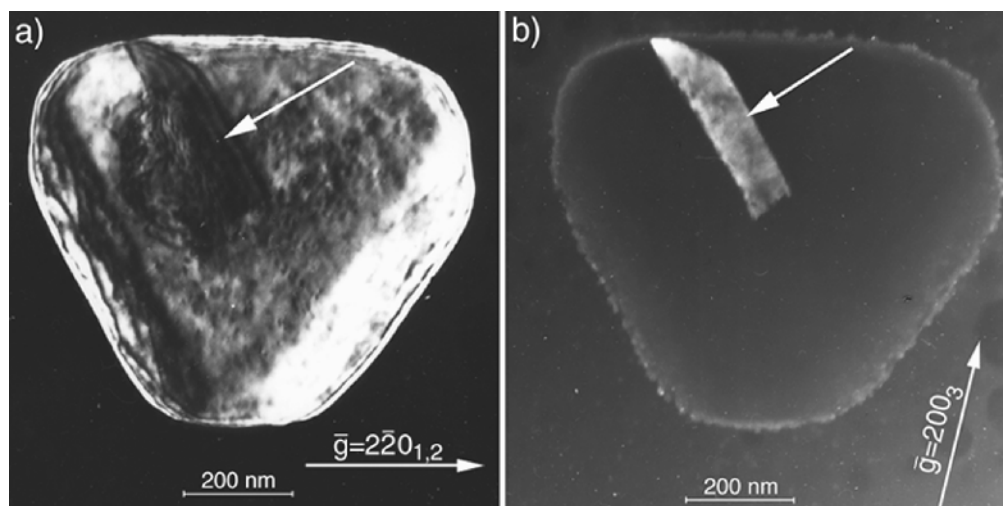It was shown that the microtwins already occur in crystals at the end of the physical ripening. Most prob-

Figure 3. a) and b) Dark field images, which show the presence of a microtwin indicated by the white arrow, using a reflection of the crystal and of the twinned variant respectively.
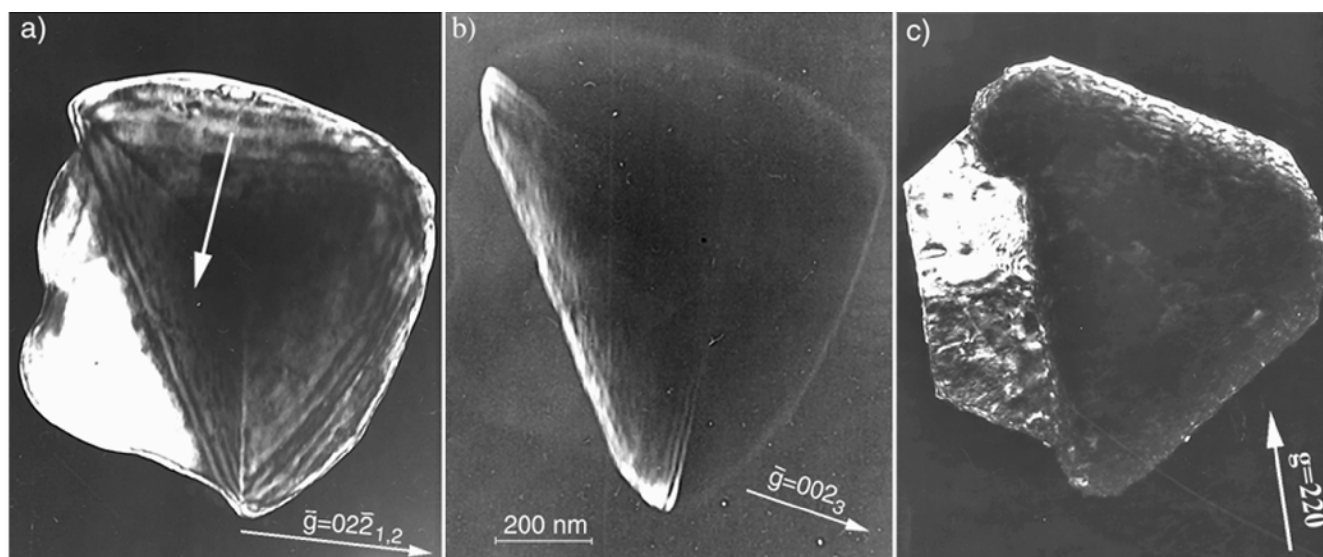

Figure 4. a) Dark field TEM image of a tricrystal using a reflection common to the first and second variant. The triangular fringe like contrast indicated by the white arrow is due to a non-parallel twin. b) Dark field TEM image using a reflection of variant 3; and c) Tricrystal with a trapezoidal part.

ably the non-parallel twins are already formed during the nucleation phase, at the same moment or immediately after the formation of the twins that induce the tabular growth.

The shape of the projection on the basal plane of the crystal in Fig. 3 is still more or less a hexagon; in most cases, however, three long and three shorter sides are formed. The thickness fringes on the side of the crystal indicate that the thickness of the top variant increases towards the center of the crystal, when observed in plan view. This yields a wedge shape, giving rise to thickness fringes as observed. These are thick tabular crystals, as confirmed by scanning electron microscopy. The SEM image also showed that the side surfaces enclose an acute angle with the basal plane, which is in practice an angle of 70.5°.

The morphology and defect structure of a fourth type of thick crystals can be deduced from the TEM images of Fig. 4. The three-dimensional morphology is that of a crystal consisting of a thick almost tetrahedral shaped part and a flat triangular or trapezoidal part. Moreover, at the transition from the thin to the thick part a triangular shaped area is observed as indicated by the white arrow in Fig. 4a. Figure 4b shows a dark field image using a beam that has been diffracted by the triangular region. This, together with the diffraction analysis, indicates that again a third twin variant is present and that the contrast is due to a twin. The morphology of this third twin variant is that of a thin slab lying on top of the tetrahedron shaped part, similar to the two twinned regions on top of the tetrahedrons in AgBr emulsions. Therefore, the terminology "tricrystal" is more appropriate than "bicrystal" as used in a previous publication,[23] and will be used from now on.

The TEM images of the flat part show no contrast indicating the presence of extra defects. This means that only planar defects parallel to the basal plane can be present. From the analysis of the diffraction patterns
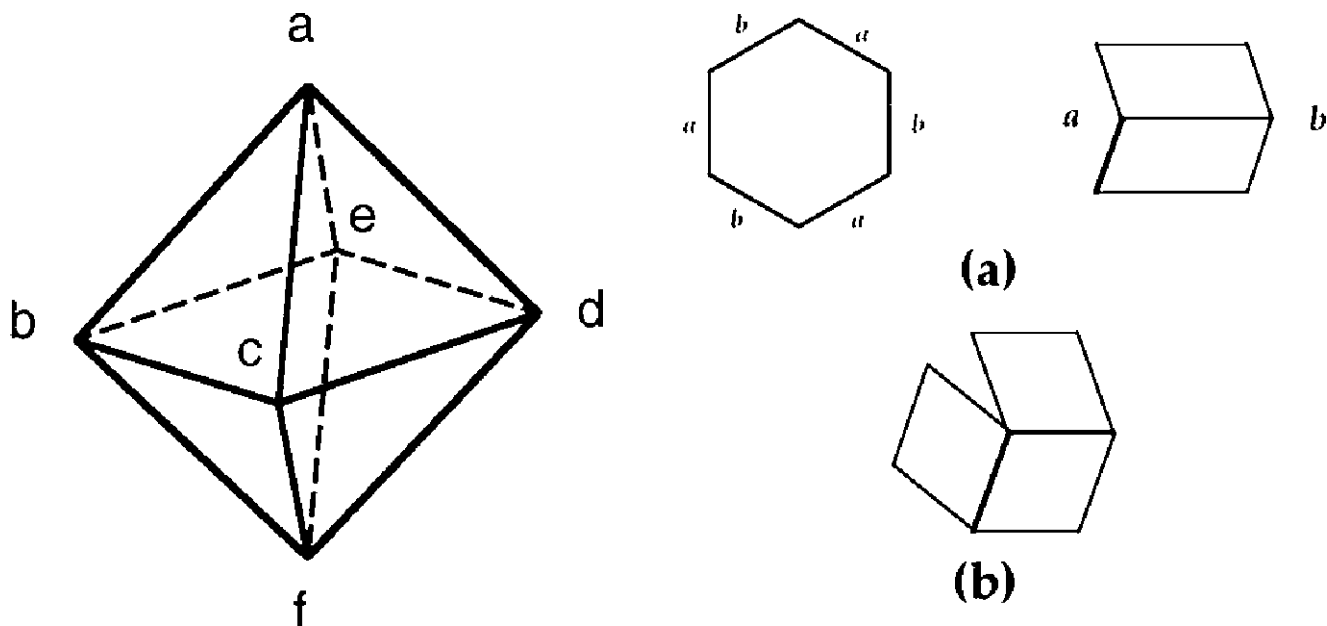
Figure 5. Schematic representation of an octahedral crystal. Twinning can occur along any {111} type plane, i.e., along abc, acd, ade, abe, bcf, bef, edf, and cdf. If twinning has occurred along the abc plane, subsequent twinning can be of three different kinds.

the presence of two twin variants in the flat part can be deduced. The shape of the flat part of the crystals, projected on the (111) basal plane, varies from a triangle (Fig. 4a) to a trapezoid (Fig. 4c). Due to the dissolution of the crystal, the edges of the flat part are also often rounded, sometimes troubling the determination of their direction, as in Fig. 4a. Occasionally, a well-configured tricrystal is observed as in Fig. 4c. For those, a typical half hexagon is formed always limited by [110] traces. This also indicates that the edge planes of the flat part of the crystal are {111} or {100} planes, like for the tetragonal part.

Growth Models in the Presence of Multiple Twinning

In the following growth models will be presented that account for the observed morphologies. From the present observations it is not possible to determine if {100} as well as {111} faces are present. This issue will not be discussed here because on a qualitative level, the same conclusions can be drawn when accelerated growth is due to the presence of small {100} faces or to the occurrence of re-entrant corners formed at the intersection of the twin planes with the side faces.

Silver Bromide. Twinning in AgBr and AgCl crystals can be described in a general way with the aid of Fig. 5, in which an octahedral crystallite is shown. Twinning can occur along any (111) type plane, i.e., along abc, acd, ade, abe, bcf, bef, edf, and cdf. If twinning has occurred along the abc plane subsequent twinning can be subdivided into three different kinds. First, the second twinning event can occur along the (111) plane parallel to the abc (111) plane, i.e., along the edf (111) type plane. This type of twinning results in tabular crystals. A second kind consists of the subsequent twinning along a (111) type plane that is connected to the abc (111) plane by a line, i.e., along abe, bcf, or acd. It should be noted
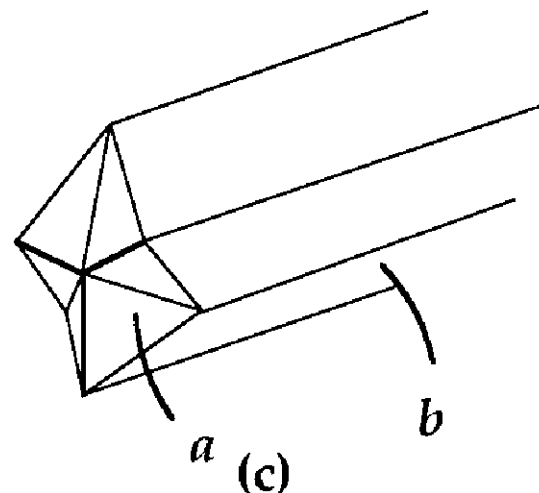

Figure 6. Schematic representation of the growth model for needle shaped crystals. After the first twinning event (a), subsequent twinning occurs along one of the {111} type planes at the fast growing sides of the crystallite, after which the situation depicted in (b) is obtained. Along the long axis of the needle, b-type sides bound the crystal, while a-type sides or {100} faces (fast growing sides) are present near the endpoints of the needle, inducing the unilateral growth.

that this is equivalent to twinning along a (111) type plane enclosing an inscribed angle of 109.5° with the abc plane. A third kind consists of the subsequent twinning along a (111) type plane that is connected to the abc (111) plane by a point, i.e., along ade, cdf, or bef which is equivalent to twinning along a (111) type plane enclosing an inscribed angle of 70.5° with the abc plane. These three groups result in three different crystal morphologies, i.e., tabular crystals, needle crystals or tetrahedral crystals.

If double twinning occurs along (111) type planes enclosing an angle of 109.5° with each other, needle shaped crystals are formed, which can be demonstrated with the aid of Fig. 6. After the first twinning event, the crystal would normally grow out to become a small triangu-

lar tabular crystal, the final size being determined by the size of the untwinned crystallite at the moment of twinning. The second twinning event, on a (111) type plane enclosing an inscribed angle of 109.5° with the first twin plane, has to occur on the *a*-sides, because these are the only sides on which (111) planes are present with the above mentioned angle (see Fig. 6a). This implies that needle shaped crystals can only be formed during the first period of nucleation during which the *a*-sides have not yet grown themselves out of existence. Once this period has elapsed, the only possible morphologies that can be formed are tabular crystals and tetrahedral crystals.

After the second twinning event, the situation as the one shown in Fig. 6b is obtained. In this figure, three octahedral crystals are shown, in twin relation with each other, the inscribed angle between the twin planes (black lines) being 109.5°. The open space in Fig. 6b is closed by rapid adsorption of new growth material, thus forming the {221} type interface. A perspective view of the crystal obtained is shown in Fig. 6c, showing the presence of re-entrant grooves at the emergence line of the three interfaces, and obtuse angles on all other crystal parts, indicating rapid unilateral growth. Moreover, the grooves do not grow out of existence, but are in fact self-perpetuating enhanced nucleation sites, thus explaining the growth behaviour. An alternative explanation was given by Bögels co-workers.[27] They argue that the tip of the needle consists of {100} surfaces while the side faces are {111} surfaces. Under the present conditions the {100} faces are rough and grow faster than the {111} side faces, inducing one-dimensional growth. The roughening of the {100} faces is also in agreement with the rounded shape of the tip of the needle as observed in Fig. 1.

The third kind of twinning is when the second twinning event takes place along a (111) type plane that encloses an inscribed angle of 70.5° with the first twin plane. This means that in Fig. 6a the second twinning event has to take place at (111) type planes of the *b*-sides. Because these sides are the non-growing sides, the effect on the growth of the two twinning events can be treated separately. The first twinning event results in a small triangular tabular crystal, as mentioned before. This is schematically depicted in Fig. 7a. The second twinning event, as is shown in Fig. 7b, results in the appearance of one re-entrant groove or {100} surface, indicated in the figure by arrows. The growth rate in the direction perpendicular to the groove and parallel to the twin plane is hereby enhanced, and a tetrahedron-like crystal morphology results, as shown in Fig. 7c and 7d. Growth is subsequently stopped due to the lack of re-entrant grooves or {100} surface; i.e., the grooves are not self-perpetuating. It should be mentioned that the effect on the growth of the two twinning events is treated separately for simplicity reasons. However, no firm evidence exists that this really is the case, i.e., the second twinning event may have happened before the situation depicted in Fig. 7a is obtained.

Silver Chloride. To account for the morphology of the thick crystals in silver chloride the same model as for silver bromide can be used. The major difference is that more twin planes parallel to the basal plane are present in these crystals.

For the thick crystals studied here, the angle between the twin planes is always 70.5° and therefore the growth model of the tetrahedrons has been adapted to explain the growth sequence. Figure 8 is a schematic represen-
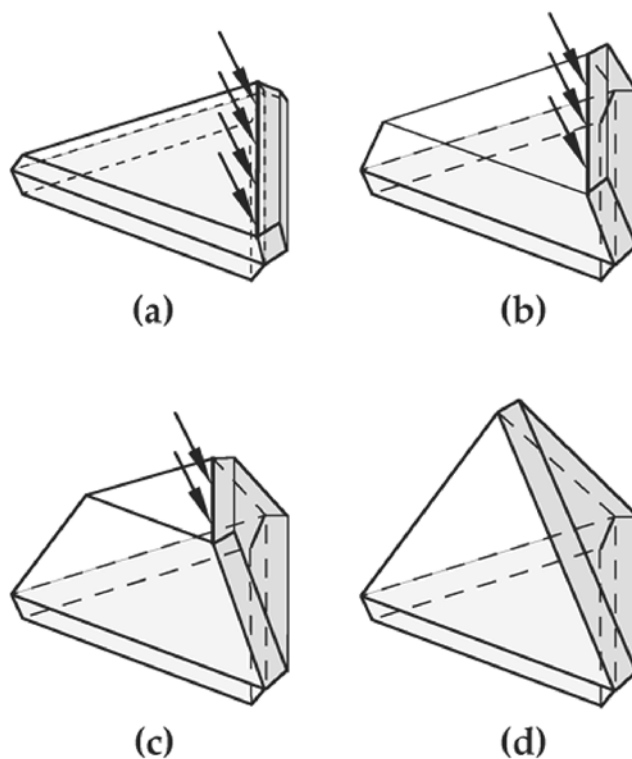

Figure 7. Schematic representation of the growth model for tetrahedral shaped crystals. After the first twinning event (light gray variant), subsequent twinning occurs along one of the {111} type planes at the slow growing sides of the crystallite (dark gray variant), after which the situation depicted in (a) is obtained. One re-entrant groove or small {100} plane is present, indicated by the arrows, along which rapid growth occurs (b–d).

tation of the proposed growth model. It is based on the assumption of two parallel tabular twin planes, because of the projected hexagonal shape of the crystals in the TEM images. Because the non-parallel microtwin has been observed in crystals after the physical ripening, it is concluded that all twins are introduced in the early stages of the growth process, i.e., when the crystals are produced under high supersaturation. First the parallel twins are introduced inducing lateral growth. On one of the side faces an accidental twin is formed that ends halfway the side face, forming an incoherent boundary (Fig. 8a). After a few layers the twinned variant is overgrown by the correctly stacked variant resulting in an internal microtwin (Fig. 8b). The microtwin induces accelerated growth of the top surface through the appearance of a small {100} face or a trough at this location (Figs. 8c and 8d) and in this way thick tabular crystals are formed.

A schematic representation of the growth model of the tricrystals is shown in Fig. 9. It starts from a nucleus with three parallel twin planes. The number of parallel twin planes could not be determined directly from our observations, but many indications have been found which confirm our proposal. On one of the slow growing side faces one non-parallel twin is formed (Fig. 9a), inducing accelerated growth in three dimensions (Figs.
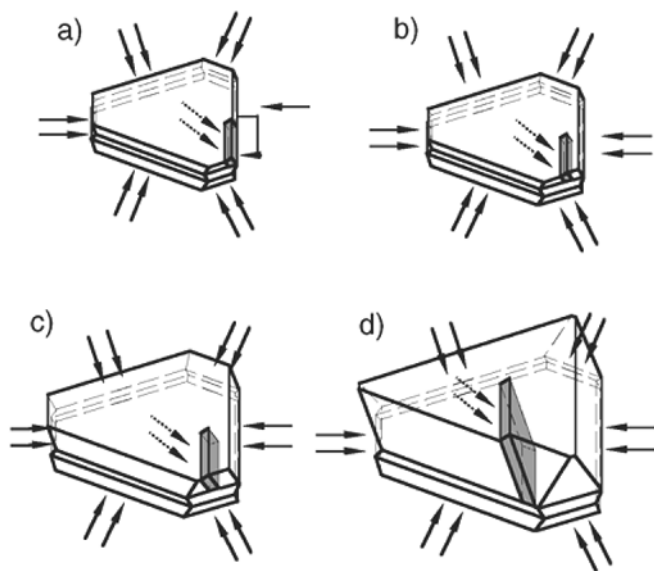
Figure 8. Successive steps in the growth of thick tabular crystals. The black arrows indicate the side faces where accelerated growth occurs. a) Nucleus with two parallel twins and one accidental twin (in gray). b) The internal microtwin is formed by overgrowth with the correctly stacked variant. c–d) Continuation of growth leads to the formation of thick tabular crystals.

Figure 9. Successive steps in the growth of the tricrystals. The black arrows indicate the surfaces where accelerated growth occurs. a) Nucleus with three parallel twins and one accidental twin (in grey). b–d) The left part of the crystal grows into a tetrahedron. Continuation of growth along the parallel twins forms the right part of the crystal. It contains only two parallel twins and grows into a trapezoidal shape.

9b–d). The non-parallel twin creates a small {100} face or a trough on the top surface, leading to the accelerated growth to culminate in the pyramidal part of the crystal. Concurrently, accelerated growth occurs along the side faces. The growth of the side faces without the non-parallel twin only enlarges the size of the tabular part. The growth of the third side face induces the extension of the flat part. While the tetrahedral part is believed to contain three parallel twin planes, the flat part contains only two parallel twin planes. Consequently, all edge planes grow at approximately the same speed. Therefore the edge planes that had disappeared in the tetrahedral part, will persist in the flat part, yielding the trapezoidal shape in Fig. 4c. Small differences in growth speed and the partial dissolution of the crystal account for the shapes observed in Fig. 4a.

A small minority of the silver chloride thick crystals have more complex twin configurations which give rise to various, less characteristic morphologies. These crystals have not been analysed in detail, but it is reasonable to assume that also in these crystals the twins are responsible for the specific morphology.

Comparison AgBr and AgCl. The origin of the formation of thick crystals in silver bromide and silver chloride emulsions is similar. In both cases it is due to the formation of twins on {111} type planes that are not parallel to the tabular plane. Yet different morphologies have been observed and this is related to the number of twins formed and the angle between the twin planes. In silver bromide only crystals containing two non-parallel {111}-type twin planes have been observed and the angle between these two planes determines the morphology. In needle crystals also a {221} interface is present, but this is the result of the twinning on the two {111} planes. For silver chloride at least three twin planes are present, lying on two non-parallel {111} planes. In
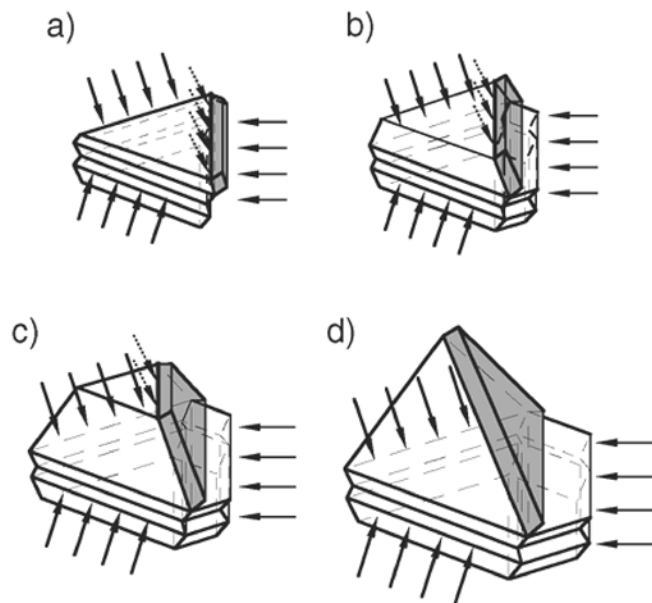
this case the number of parallel twin planes and the ending of the non-parallel twin inside the crystal are responsible for the difference in morphology.

Theoretically, it is possible that all four morphologies occur in AgBr as well as AgCl, but this was not observed under the present precipitation conditions. The reason is probably that twinning in AgCl occurs more frequently than in AgBr. Experiments in which silver bromide and chloride crystals are formed from the vapor phase[28] have shown that critical super-saturation for forming twins is comparable, but for silver chloride more needle shaped crystals and more tabular crystals with three parallel twin planes are formed. The reason for the difference in number of twins could not be explained as yet. According to the same authors, increasing the driving force will probably not produce silver bromide thick crystals with the morphologies observed in silver chloride emulsions. It was experimentally found that at higher super-saturation, twins are more easily formed, but the number of twins in one crystal is not significantly altered, as necessary for obtaining these morphologies.

Conclusion

In this study it is shown that the thickness growth of silver bromide and silver chloride tabular crystals with {111} surfaces is caused by the formation of non-parallel twins. In both AgBr and AgCl two morphologies occur more often. In AgBr needles and tetrahedron shaped crystals are formed, while in AgCl thick crystals with an "incomplete" microtwin and crystals consisting of a tetrahedral shaped part and a flat triangular to trapezoidal part occur. Growth models have been proposed for all observed morphologies, with the major differences being the angle between the twin planes and the number of twin planes that are present. The reason for observing only

two morphologies in AgBr as well as AgCl is related to the experimental observation that above a critical super-saturation twinning occurs more frequently in silver chloride than in silver bromide. ⚠

References

1. R. Jagannathan, *J. Imaging Sci.* **35**, 104 (1991).
2. R. Jagannathan and V. V. Gokhale, *J. Imaging Sci.* **35**, 113 (1991).
3. C. R. Berry and D. C. Skillman, *Photogr. Sci. Eng.* **6**, 159 (1962).
4. J. F. Hamilton and L. E. Brady, *J. Appl. Phys.* **35**, 414 (1964).
5. D. Shechtman, J. L. Hutchison, L. H. Robins, E. N. Farabaugh, and A. Feldman, *J. Mater. Res.* **8**, 473 (1993).
6. D. Shechtman, A. Feldman and J. Hutchison, *Mater. Lett.* **17**, 211 (1993).
7. J. C. Angus, M. Sunkara, S. R. Sahaida, and J. T. Glass, *J. Mater. Res.* **7**, 3001 (1992).
8. J. Li, T. Mitsuki, M. Ozawa, H. Horiuchi, K. Kishio, K. Kitazawa, K. Kikuchi, and Y. Achiba, *J. Cryst. Growth* **143**, 58 (1994).
9. A. I. Kirkland, D. A. Jefferson, D. G. Duff, and P. P. Edwards, Inst. Phys. Conf. Ser. No. 98, paper presented at EMAG-MICRO 89, Institute of Physics, London, 1989, Chap. 8, p. 375.
10. D. R. Hamilton and R. G. Seidensticker, *J. Appl. Phys.* **31**, 1165 (1960).
11. R. Jagannathan, R. V. Mehta, J. A. Timmons, and D. L. Black, *Phys. Rev. B*, **48**, 13261 (1993).
12. N.-B. Ming and I. Sunagawa, *J. Cryst. Growth* **87**, 13 (1988).
13. N.-B. Ming and H. Li, *J. Cryst. Growth* **115**, 199 (1991).
14. R. V. Mehta, R. Jagannathan and J. A. Timmons, *J. Imaging Sci. Technol.* **37**, 107 (1993).
15. N.-B. Ming, *J. Cryst. Growth* **128**, 104 (1993).
16. G. Bögels, T. M. Pot, H. Meekes, P. Bennema, and D. Bollen, *Acta Cryst.* **A53**, 84 (1997).
17. Y. Hosoya and S. Urabe, A Study on the Mechanism of Nucleation and Growth of Twin Tabular AgBr Crystals, in *Proc. of 1997 International Symposium on Silver Halide Imaging*, IS&T, Springfield, VA, 1997, p. 22.
18. W. Van Renterghem, C. Goessens, D. Schryvers, J. Van Landuyt, P. Verrept, D. Bollen, C. Van Roost, and R. De Keyzer, *J. Cryst. Growth* **187**, 410 (1998).
19. F. H. Claes, J. Libeer and W. Vanassche, *J. Photgr. Sci.* **21**, 39 (1973).
20. K. Endo and M. Okaji, *J. Photgr. Sci.* **36**, 182 (1988).
21. C. Goessens, D. Schryvers, J. Van Landuyt, A. Millan, and R. De Keyzer, *J. Cryst. Growth* **151**, 335 (1995).
22. C. Goessens, D. Schryvers, J. Van Landuyt, and R. De Keyzer, *J. Cryst. Growth* **172**, 426 (1997).
23. W. Van Renterghem, D. Schryvers, J. Van Landuyt, D. Bollen, C. Van Roost, and R. De keyzer, *J. Imaging Sci. Technol.* **45**, 83 (2000).
24. G. Bögels, H. Meekes, P. Bennema, and D. Bollen, *to* be submitted.
25. C. Goessens, D. Schryvers, J. Van Landuyt, S. Amelinckx, A. Verbeeck, and R. De Keyzer, *J. Cryst. Growth* **110**, 930 (1991).
26. S. Chen, S. Jagannathan, R. V. Mehta, R. Jagannathan, and A. E. Taddei, Direct observation of Stacking Fault Structure in (111) Tabular Silver Halide Grains by High-Resolution Electron Microscopy, in *Proc. of 1997 International Symposium on Silver Halide Imaging,* IS&T, Springfield, VA, 1997, p. 44.
27. G. Bögels, J. G. Buijnsters, S. A. C. Verhaegen, H. Meekes, P. Bennema, and D. Bollen, *J. Cryst. Growth* **203**, 554 (1999).
28. G. Bögels, H. Meekes, P. Bennema, and D. Bollen, *Phil. Mag. A* **79**, 639 (1999).